

Identification of Lead Moiety to Treat Polycystic Ovarian Syndrome from *Ganoderma lucidum*: A Computational Approach

Manisha Devi ^{1,*} , Gandaboyana Chaitanya Sai ², Damodar Nayak Ammunje ¹, Parasuraman Pavadai ², Selvaraj Kunjiappan ³, Anbu Jayaraman ^{1,*} 

¹ Department of Pharmacology, Faculty of Pharmacy, M S Ramaiah University of Applied Sciences, Bengaluru-560054, Karnataka, India

² Department of Pharmaceutical Chemistry, Faculty of Pharmacy, M S Ramaiah University of Applied Sciences, Bengaluru-560054, Karnataka, India

³ Department of Biotechnology, Kalasalingam Academy of Research and Education, Krishnankoil-626126, Tamilnadu, India

* Correspondence: manisha1996.mc1@gmail.com (M.D.); anbucolegist@gmail.com (A.J.);

Scopus Author ID 57207890209

Received: 18.08.2022; Accepted: 30.10.2022; Published: 24.12.2022

Abstract: Polycystic ovarian syndrome (PCOS) is characterized by gynecological, endocrine, and metabolic abnormalities in women of reproductive ages. Symptoms include hypergonadotropism, amenorrhea, oligomenorrhea, multiple cysts in ovaries, hirsutism, obesity, and commonly associated with infertility. Presently the standard treatment for PCOS includes lifestyle modifications, pharmacological treatments, and surgical procedures. However, these treatments are not promising for the complete elimination of PCOS. Therefore, natural sources have been a highly valued source of medicine and help improve and manage PCOS conditions. *Ganoderma lucidum* (*G.lucidum*) is an oriental fungus possessing a wide range of medicinal properties. Ganoderic acids (GAs) have been reported to show antioxidant, anti-cancer, anti-diabetic, anti-inflammatory, anti-hyperlipidemic, immunomodulatory, and antiandrogenic effects. Molecular docking studies for 22 GAs and clomiphene with human androgen receptor (PDB ID: 1E3G) were carried out using AutoDock Vina and PyRx 0.8 tool. ADMET analysis was carried out for the top 5GAs using pkCSM to predict small molecule pharmacokinetic and toxicity properties. The stability of protein-ligand complex GAA-1E3G was analyzed using Desmond. The binding affinity of Ganoderma triterpenes with 1E3G ranged from -6.9 to -8.7 kcal mol⁻¹. Ganoderic acid A showed a maximum affinity with a score of -8.7, unlike standard drugs with a score of -6. The *in silico* predicted pharmacokinetic properties of the top 5 ganoderic acids were better when compared to standard drugs with minimum toxicity. The stability of GAA at 1E3G binding pockets was validated using molecular dynamics. Hence, GAA can be further evaluated for the successful treatment of PCOS.

Keywords: PCOS; *Ganoderma lucidum*; ganoderic acids; molecular docking; molecular dynamics.

© 2022 by the authors. This article is an open-access article distributed under the terms and conditions of the Creative Commons Attribution (CC BY) license (<https://creativecommons.org/licenses/by/4.0/>).

1. Introduction

Polycystic ovarian syndrome (PCOS), going by the name of Stein-Leventhal [1] syndrome, is characterized by gynecological, endocrine, and metabolic abnormalities in women at reproductive ages [2,3]. A "string of pearls" [4] like structure is seen in polycystic ovaries due to an abnormal number of eggs developing in the ovarian periphery. Symptoms

include hypergonadotropism, amenorrhea, oligomenorrhea, multiple cysts in ovaries, hirsutism, obesity, and commonly associated with infertility [2]. Multiple metabolic abnormalities, such as insulin resistance, hyperinsulinemia, impaired glucose tolerance, endothelial dysfunction, hypertension, and dyslipidemia, are also involved, increasing the risk of diabetes and cardiovascular disease [2].

According to World Health Organization, PCOS affected around 3.4% of women worldwide in 2012 [5,6]. The commonness of PCOS is exceptionally factored in all around the world, and it ranges from around 2.2% to 26% [6]. According to Liu *et al.*, there were 1.55 million incident cases of PCOS among women of reproductive age (15-49 years) worldwide in 2017, up 4.47 percent from 2007 [7]. In India, the prevalence rate of PCOS varies from region to region. According to a study by Nidhi *et al.*, PCOS's prevalence was 9.13% in girls between 15 and 18 years of age [8]. Bharthi *et al.* established the prevalence of PCOS in India was 6%, and the prevalence of PCOS was higher in the urban population when compared to the rural population [5]. Gupta *et al.* reported a prevalence of 8.2% in Bhopal [6]. A study carried out by Bashir *et al.* showed a 10% prevalence of PCOS in women [9].

Androgen excess is the major predisposing factor for PCOS. LH levels are typically increased due to elevated total free testosterone [1]. High androgen levels also inhibit the development and maturation of the ovarian follicles [1,10]. DHEA levels are also increased in 50-75% of women with PCOS, which contributes to increased androgen levels [1,10,11]. Androgen excess also contributes to the increase in body weight [1,12]. Also, the main cause of hirsutism in PCOS women has increased androgen [10,11,13]. Insulin resistance is reported in 50-70% of women with PCOS [11], and 30-40% of obese women with PCOS have been reported for diabetes and impaired glucose tolerance [8]. PCOS and insulin resistance are interrelated endocrine disorders. Obesity, poor diet, and stress are the common causes of insulin resistance [1]. Insulin resistance results in hyperinsulinemia, which is an important pathology of PCOS, by stimulating ovarian testosterone production, decreasing serum SHBG, and impending ovulation [14]. PCOS women with a family history of diabetes mellitus depict impaired β -cell function [11]. IR and hyperinsulinemia play an important role in the pathogenesis of the pituitary-ovarian axis [12]. Obesity increases IR, which contributes to the increase of testosterone, decreases gonadotropin production and is also associated with anovulation [10,12]. Insulin collaborates with LH and also decreases SHBG, causing an increase in free serum testosterone. Hyperinsulinemia amplifies FSH-induced upregulation of LH receptors in granulosa cells, which seizes cell proliferation and follicle growth [10]. In women with PCOS, follicular growth is disrupted due to hyperandrogenism, insulin resistance, and altered intraovarian paracrine signaling. The increased aromatase expression in granulosa cells in the antral follicles causes follicular arrest in PCOS women [11,14]. Increased LH stimulates theca cell hyperandrogenism, and decreased FSH inhibits the expansion of follicular size and maturity [10]. In PCOS, the follicular arrest is accompanied by oligomenorrhea, amenorrhea, anovulation, sub-fertility and peripheral accumulation of antral follicles in the ovaries providing a polycystic morphology [11]. Obesity affects 80 percent of PCOS patients and is associated with multiple metabolic complications like dyslipidemia, T2DM and cardiovascular risks [13]. Increased calorie intake impairs the capacity of adipose tissue stores to expand in PCOS women with insulin resistance which may partially represent dysfunctional adipogenesis [10,12]. Other predisposing factors contributing to PCOS are estrogen abnormality, gonadotropin abnormalities, hypothalamic-pituitary-adrenal axis abnormalities, and genetic and environmental factors [1,10,11,13].

Presently the standard treatment for PCOS includes lifestyle modifications and pharmacological treatments. Lifestyle modifications are the first treatment line, including diet, exercise, and weight loss. Restriction of calorie consumption, taking part in daily exercise, addressing behavior, undergoing pharmacological treatment, and quitting smoking and alcohol consumption [15-17]. Oral contraceptive (OC) medicines are the primary treatment options for prolonged control of PCOS. They contain estrogens and progesterone, which decrease androgen production and regulate estrogens. The formation and maturation of ovarian follicles are suppressed by estrogen, which acts by inhibiting FSH, and ovulation is suppressed by progesterone inhibiting LH [16,18]. Clomiphene citrate (CC), a selective estrogen receptor modulator, increases the secretion of FSH and LH, stimulating the growth of the ovarian follicle and thus initiating ovulation. Letrozole (LE) blocks the transformation of androgens to estrogens by inhibiting aromatase enzymes in the follicles. Metformin reduces glycogen production and improves the symptoms of high testosterone; it also inhibits glucose metabolism and inhibits follicular membrane cells. In addition, it helps to improve insulin resistance and lowers insulin levels [16-19]. Spironolactone blocks the effects of androgen on the skin and significantly reduces hirsutism after long-term treatment [16,20]. Eflornithine slows facial hair growth in women when applied topically [16]. Flutamide, an antiandrogenic drug that acts by inhibiting the conversion of testosterone to more active dihydro-testosterone, also helps improve hirsutism in PCOS women [16,19]. Laparoscopic ovarian drilling is a surgical procedure that triggers ovulation in PCOS women [21]. Bariatric surgery is the most durable and effective treatment for morbid obesity and improves metabolic syndrome [22].

Existing treatment approaches to PCOS are limited due to the prevalence of contraindications in PCOS women, treatment failure in some circumstances, and may cause severe side effects. Norethindrone or ethinylloestradiol, the primary OCs used for PCOS treatment, causes venous thrombosis [20]. Spironolactone occasionally causes fatigue, postural hypertension, and dizziness [16]. Flutamide is less used due to its high cost and hepatocellular toxicity [16]. Lactic acidosis is a major side effect of metformin, making it relatively unsafe.

Herbs have been a highly valued source of medicine throughout human history since the knowledge and usage of plants are of divine origin. Medicinal plants help improve and manage PCOD conditions. These plants help improve hyperandrogenism, insulin sensitivity, fertility, and menstrual cycles. Some of the herbs used for treating PCOS and associated disorders are- *Panax ginseng*, *Tribulus terrestris*, *Gymnema sylvestre*, *Punicagranatum*, *Aloe barbadensis*, *Cinnamomum zeylanicum*, *Glycyrrhiza glabra*, *Symplocos racemosa*, *Linum usitatissimum*, *Curcuma longa*, *Cocus nucifera*, *Foeniculum vulgare*, *Trigonellafoenum graecum*, *Camellia sinensis*, *Berberine*, *Vitex agnus-castus*, *Mentha spicata*, *Paeonia lactiflora*, *Piper nigrum*, *Piper longum*, *Commiphoramukul*, *Zingiber officinale* [1,2,23-27].

Ganoderma lucidum (*G.lucidum*) is an oriental fungus possessing a wide range of medicinal properties. It is a large, dark mushroom with a glossy exterior and a woody texture. In traditional Chinese medicine, it is referred to as an "herb of spiritual potency" and has been used for over 2000 years [28]. They are rich in polysaccharides, triterpenoids, sterols, proteins, and peptides. Ganoderic acid A (GAA), also known as Ganoderate A, belongs to the triterpene family of organic compounds. There are six isoprene units in these terpene molecules. Ganoderic acid A is a chemical molecule that is exceedingly basic (almost neutral) (based on its pKa). Ganoderic acid A has been reported to show antioxidant, anti-cancer, anti-diabetic, anti-inflammatory, anti-hyperlipidemic, anti-cyst, immunomodulatory, anti-tumor, and antiandrogenic effects [28-36].

Computer-assisted drug development (CADD) is a new method that combines mathematical modeling and simulation to accelerate drug development. This method provides a knowledge-based decision-making tool for alternative development methods based on assessing prospective medication safety concerns and the definition of future trial experimental designs with estimated power and success probabilities [37]. The process of drug discovery and development is time-consuming and costly. To bring a drug to market, it takes an average of 10–15 years and \$500–800 million [38]. The major components of CADD are homology modeling, molecular docking, virtual or high-throughput screening, quantitative structure-activity relationship, and 3D pharmacophore mapping. Docking approaches include rigid ligand and rigid receptor docking, flexible ligand and rigid receptor docking, and flexible ligand and flexible receptor docking [39,40]. This study aims to identify the lead moiety to treat polycystic ovarian syndrome using *Ganoderma lucidum* triterpenoids using molecular docking, ADMET properties, and molecular dynamics.

2. Materials and Methods

2.1. Protein preparation.

The X-ray crystallographic structure of the androgen receptor (PDB ID: 1E3G) was provided by the RCSB Protein Data Bank (<http://www.rcsb.org/pdb>) [41]. Swiss- PDB Viewer v4.1.0 was used to clean and insert the missing residues in the protein before analysis. Further, BIOVIA discovery studio version 4.0 software was used to establish the structure of the protein and amino acid positions from active regions; these were further used for docking study.

2.2. Retrieval and preparation of active compounds.

Ganoderma lucidum consists of around 250 triterpenoids which are segregated into compounds including ganoderic acids, ganoderiol, ganoderone, ganolactone, and ganoderal [42]. A group of twenty-two ganoderic acids (GAs) was selected for this study, along with clomiphene citrate as a standard drug used for the treatment of PCOS. Ganoderic acids and standard drugs were obtained with the help of the data repository (<https://cb.imsc.res.in/imppat/home>) [43], previously published literature, and PubChem (<https://pubchem.ncbi.nlm.nih.gov/>).

2.3. Molecular docking.

This approach is a pivotal part of structural biology research, and it is one of the most often-used methodologies in the drug design process. A molecular docking study was conducted using PyRx 0.8 tool [44] and the AutoDock Vina program [45]. The androgen receptor (PDB ID: 1E3G) was used as the protein, and the selected bioactive components were used as ligands. PyRx software was also used to introduce the Kollam partial charges and Polar hydrogen atoms into the 3D structures. Further, the receptor and ligand files were stored in "pdbqt" format to calculate the docking energy affinities. Each ligand's energy affinity values were computed by AutoDock Vina using up to ten distinct docking sites. The 2D and 3D structures of the complex were generated by Discovery Studio Visualizer, which also depicted the number of hydrogen bonds and non-covalent interactions for every complex [46].

2.4. Prediction of *in silico* physicochemical and pharmacokinetic properties.

The integrity and efficiency of the selected bioactive components can be determined by the *in silico* prediction of physicochemical and ADMET properties. Properties like molecular weight, surface area, rotatable bonds, water solubility, intestinal absorption, skin permeability, p-glycoprotein activity, VD_{ss}, brain permeability, metabolisms through CYP450, total clearance, AMES toxicity, maximum tolerated dose, hERG inhibitors, oral rat acute and chronic toxicity, hepatotoxicity and skin sensitization of the selected components have been determined using pkCSM pharmacokinetics web-based server (<http://biosig.unimelb.edu.au/pkcsm/prediction>) [47].

2.5. Molecular dynamics simulation.

The binding stability, conformation, and interaction mechanisms between the identified bioactive chemicals and receptor (1E3G) were determined using molecular dynamic simulation [48]. The ligand-receptor complex was subjected to molecular dynamics simulation using the DESMOND v3.6 package [49]. Furthermore, using the pre-set SCP water model, a water model was developed at a distance of 10Å units of orthorhombic period boundary [50]. Further, the electric charges were neutralized by adding the necessary amount of counter ions, and before the molecular dynamic simulation process began, the system decreased its energies through the heating and equilibrium process. The system production step lasted 100ns, with time steps of 0.001ps; 300K temperature and 1 atmospheric pressure were used with the Nose-Hoover method and the NPT (isothermal-isobaric) ensemble [51,52]. The best confirmations were chosen based on the interactions and dynamic features of the complex.

3. Results and Discussion

The aim of this study was to look at the impact of *Ganoderma lucidum* active constituents in the prevention and treatment of PCOS using pharmacoinformatics. Pharmacoinformatics is a collection of *in silico* molecular modeling methods for screening bioactive chemicals for binding affinities, pharmacokinetics, and pharmacodynamic properties [53]. Pharmacoinformatics has increased the discovery of bioactive chemicals by allowing researchers to refine the biological and synthetic research impacts. Pharmacoinformatics research was used to anticipate the favorable effects of certain drugs, which were later confirmed *in vitro* and *in vivo*. Researchers may be able to uncover therapeutic solutions for certain disease states if they can figure out how compounds bind, interact, and inhibit/ excite a protein. Initially, the androgen receptor (AR), which is linked to the PCOS phenotype and may also be involved in folliculogenesis [54], was determined to be a bioactive substance's target. In women with hyperandrogenic PCOS, serum levels of testosterone (T) and dehydroepiandrosterone sulfate (DHEAS), as well as 3-hydroxysteroid dehydrogenase (3-HSD), which is an enzyme that converts pro-androgens to bioactive androgens, are all increased [55]. The purpose of this research work was to inhibit the androgen receptor involved in hyperandrogenism by using bioactive components found in *Ganoderma lucidum* for the treatment of PCOS.

3.1. Retrieval of bioactive compounds and preparation.

A literature review was conducted to search for the triterpenoids in *Ganoderma lucidum*. Among more than 250 triterpenoids, the most accessible bioactive components were selected particularly the ganoderic acids (GAs) group [42]. A list of twenty-two bioactive components and one standard drug for PCOS were selected for this study. A similar computational study was carried out for *Ganoderma lucidum* active constituents as inhibitors against HIV protease and tyrosinase [56].

3.2. Molecular docking studies.

Molecular docking analysis was carried out to investigate the intermolecular interaction between the bioactive components and target proteins. Twenty-two bioactive components and a standard drug were docked against an androgen receptor (1E3G) using AutoDock Vina to analyze their binding capacity. Following molecular docking, the binding energies of bioactive components were found to be ranging from $-6.9 \text{ kcal mol}^{-1}$ to $-8.7 \text{ kcal mol}^{-1}$ and are illustrated in Table 1. The top five components were selected for further research, which include ganoderic acid A (GAA) $-8.7 \text{ kcal mol}^{-1}$, ganoderic acid K (GAK) $-8.3 \text{ kcal mol}^{-1}$, ganoderic acid C1 (GAC1) $-8.2 \text{ kcal mol}^{-1}$, ganoderic acid M (GAM) $-8.2 \text{ kcal mol}^{-1}$, ganoderic acid I (GAI) $-8.2 \text{ kcal mol}^{-1}$, based on their binding energies with the amino acid residues in the active site of 1E3G and is illustrated in Table 2.

Table 1. Ganoderic acids and their binding affinity against the androgen receptor.

SL.NO	Compound Name	Compound Code (CID)	Docking Scores (kcal mol^{-1})
1	Ganoderic Acid A	471002	-8.7
2	Ganoderic Acid B	471003	-7.8
3	Ganoderic Acid C1	471004	-8.2
4	Ganoderic Acid C2	57396771	-7.8
5	Ganoderic Acid C6	57396921	-8.2
6	Ganoderic Acid D	102004379	-7.2
7	Ganoderic Acid E	10075137	-7.2
8	Ganoderic Acid F	23247895	-7.6
9	Ganoderic Acid G	73657193	-7.4
10	Ganoderic Acid H	73657194	-8.2
11	Ganoderic Acid I	20055990	-8.2
12	Ganoderic Acid J	20055991	-7.7
13	Ganoderic Acid K	74036828	-8.3
14	Ganoderic Acid M	5317490	-8.2
15	Ganoderic Acid N	131751706	-7.6
16	Ganoderic Acid L	101600071	-7.9
17	Ganoderic Acid S	12444571	-6.9
18	Ganoderic Acid T	21637704	-7.5
19	Ganoderic Acid AM1	10346401	-7.3
20	Ganoderic Acid Lm2	11813266	-7.9
21	Ganoderic Acid DM	11784642	-7.1
22	Ganoderic Acid α	471001	-7.5
23	Standard	2800	-6

Table 2. Ganoderic acids with maximum docking score.

SL.NO	Compound Name	Docking Score
1	Ganoderic Acid A	-8.7
2	Ganoderic Acid K	-8.3
3	Ganoderic Acid C1	-8.2
4	Ganoderic Acid M	-8.2
5	Ganoderic Acid I	-8.2

3.3. Interpretation of protein-ligand interactions.

BIOVIA discovery studio visualizer tool was used to anticipate the interactions between the five selected components and 1E3G. It was observed that GAA (CID-471002) showed maximum interaction with 1E3G with the binding energy of $-8.7 \text{ kcal mol}^{-1}$. GAA formed two conventional hydrogen bond interactions with SER782P and ARG779P, eleven VanDer Waals interactions with ASP879P, PHE876P, GLN783P, MET780P, HSD776P, TYR781P, VAL887P, PHE697P, LEU701P, LYS883P and LEU880P, and one alkyl interaction with ARG779P the active site amino acid residues of 1E3G respectively showed in Figure 1 and Table 3. GAK (CID-74036228) showed sixteen VanDer Waals interactions THR755P, ASN766P, ARG752P, GLY683P, VAL684P, PRO682P, GLN711P, VAL685P, PHE764P, PRO766P, ALE765P, PHE804P, GLU681P, ALA748P, LEU805P, PRO801P and GLN802P, one conventional hydrogen bond interaction GLU678P, and one carbon hydrogen bond interaction TRP751P with the amino acid residues of 1E3G respectively as depicted in Figure 2 and Table3. GAC1 (CID-471004) showed eleven VanDer Waals interactions ALA748P, GLY683P, ARG752P, PHE804P, TRP751P, THR755P, PRO801P, GLN802P, GLU678P, LEU805P and LYS808P, one conventional hydrogen bond interaction GLU781P, and three alkyl interactions VAL648P, VAL685P and PRO682P with the amino acid residue of 1E3G respectively as depicted in Figure 3 and Table 3. GAM (CID-5317490) showed twelve VanDer Waals interactions GLU678P, LEU805P, GLU681P, GLY683P, ALA748P, HSD714P, VAL715P, GLN711P, THR755P, PHE804P, PRO801P and GLN802P, three conventional hydrogen bond interactions LYS808P, ARG752P and TRP751P, and three alkyl interactions VAL684P, VAL685P and PRO682P with the amino acid residue of 1E3G respectively as depicted in Figure 4 and Table 3. GAI (CID-10075137) showed five conventional hydrogen bond interactions ARG752P, GLU681P, GLU678P, GLN802P, and LYS808P, and four alkyl interactions PRO682P, VAL685P, PRO801P, and TRP751P with the amino acid residue of 1E3G respectively as depicted in Figure 5 and Table 3. The standard drug for PCOS (CID-2800) showed three alkyl interactions, ALA748P, ARG752P, and LEU805P, and one Pi-anion interaction GLU681P with the amino acid residue of 1E3G, respectively, as depicted in Figure 6 and Table 3.

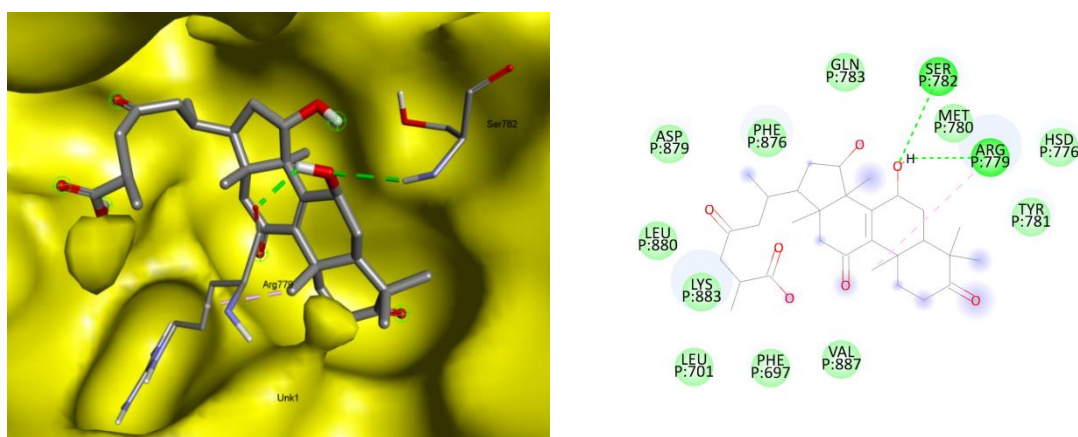


Figure 1. The interaction between GAA (CID-471002) and 1E3G. The left figure represents 3D, and the right figure represents 2D complex protein-ligand interaction.

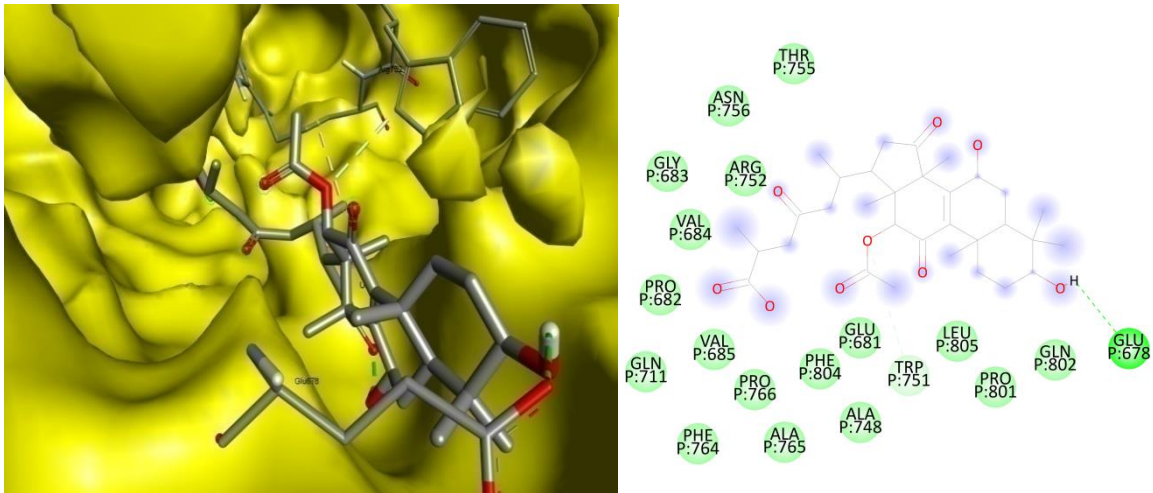


Figure 2. The interaction between GAK (CID-74036828) and 1E3G. The left figure represents 3D, and the right figure represents 2D complex protein-ligand interaction.

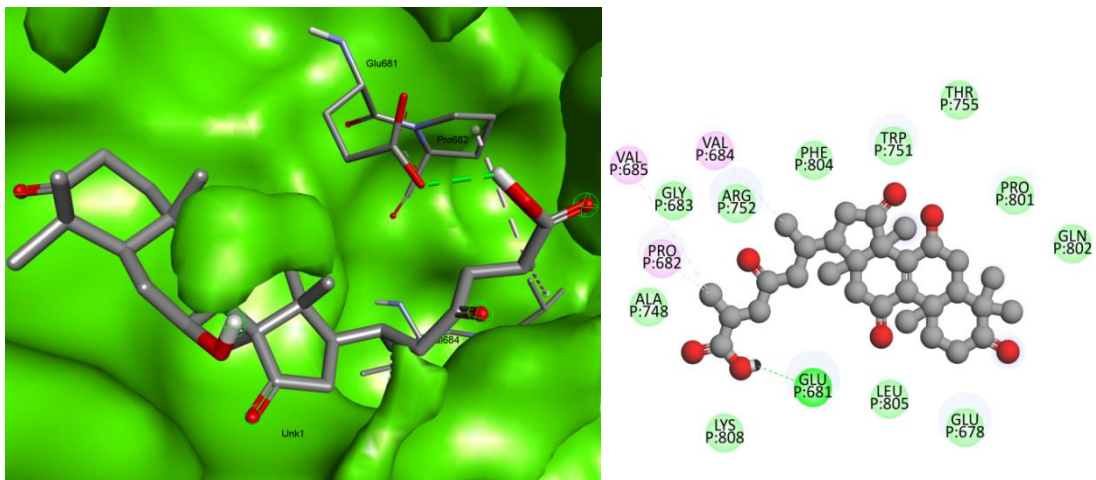


Figure 3. The interaction between GAC1 (CID-471004) and 1E3G. The left figure represents 3D, and the right figure represents 2D complex protein-ligand interaction.

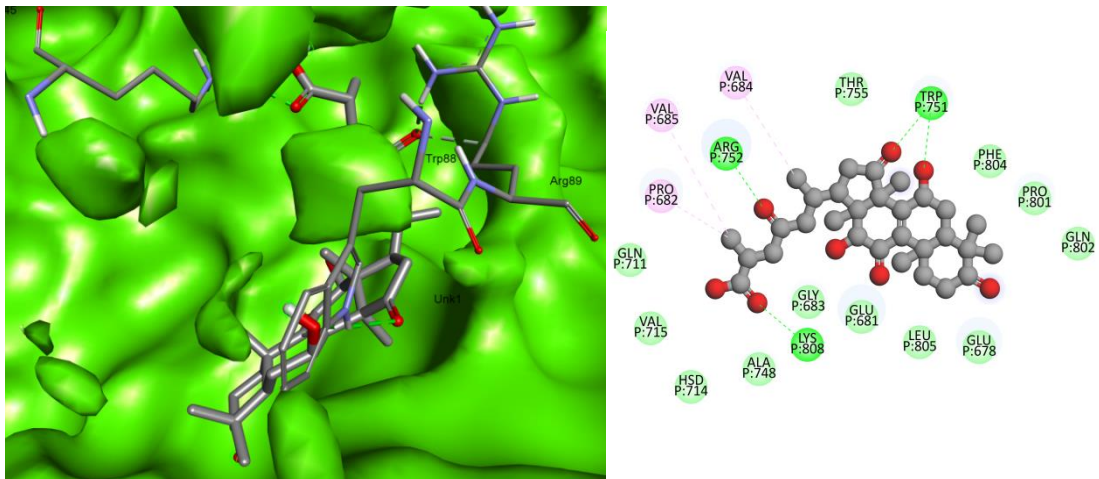


Figure 4. The interaction between GAM (CID-5317490) and 1E3G. The left figure represents 3D, and the right figure represents 2D complex protein-ligand interaction.

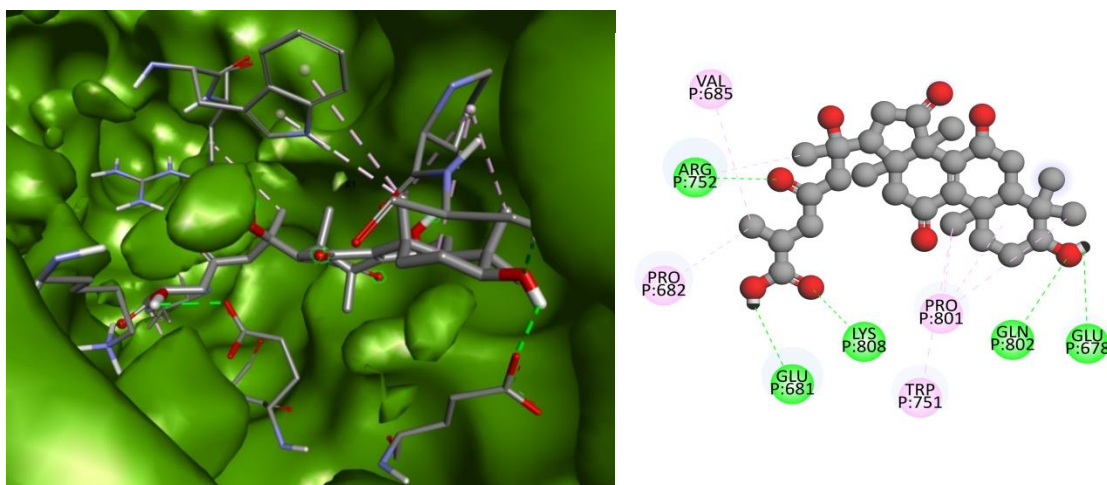


Figure 5. The interaction between GAI (CID-10075137) and 1E3G. The left figure represents 3D, and the right figure represents 2D complex protein-ligand interaction.

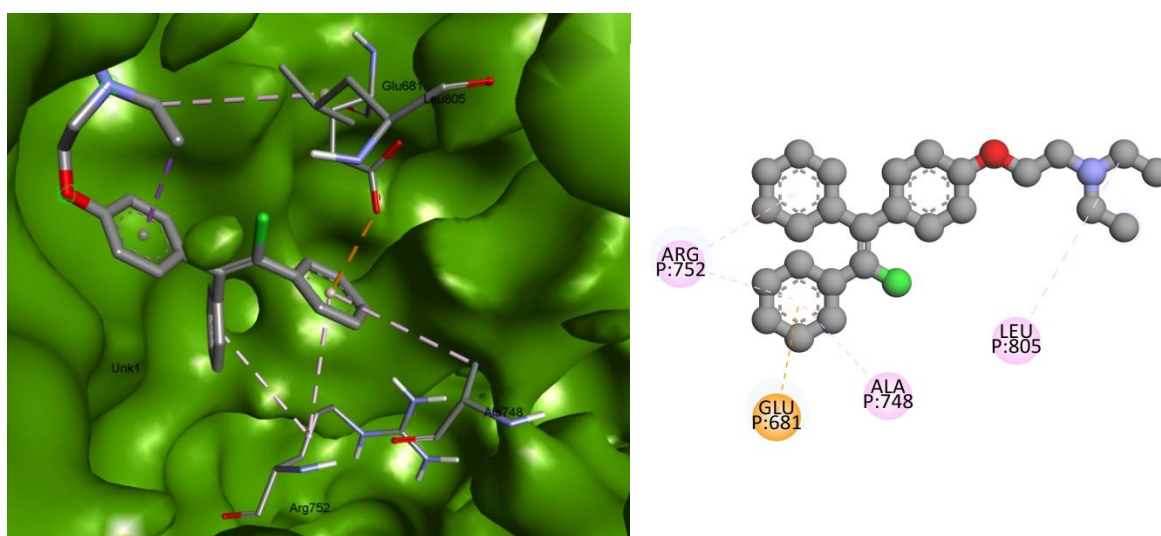


Figure 6. The interaction between standard drug (CID-2800) and 1E3G. The left figure represents 3D, and the right figure represents 2D complex protein-ligand interaction.

Table 3. List of bonding interactions between selected 5 bioactive compounds and standard with the androgen receptor.

Compound Name	Residues	Amino Acids	Bond Category
Ganoderic acid A CID-471002	782P	SER	Conventional Hydrogen Bond
	779P	ARG	Conventional Hydrogen Bond
	779P	ARG	Alkyl
	879P	ASP	Van Der Waals
	876P	PHE	Van Der Waals
	783P	GLN	Van Der Waals
	780P	MET	Van Der Waals
	776P	HSD	Van Der Waals
	781P	TYR	Van Der Waals
	887P	VAL	Van Der Waals
	697P	PHE	Van Der Waals
	701P	LEU	Van Der Waals
	883P	LYS	Van Der Waals
	880P	LEU	Van Der Waals
Ganoderic acid K CID- 74036828	678P	GLU	Conventional Hydrogen Bond
	751P	TRP	Carbon Hydrogen Bond
	752P	ARG	Alkyl
	755P	THR	Van Der Waals
	756P	ASN	Van Der Waals
	683P	GLY	Van Der Waals
	684P	VAL	Van Der Waals
	682P	PRO	Van Der Waals

Compound Name	Residues	Amino Acids	Bond Category
	711P	GLN	Van Der Waals
	685P	VAL	Van Der Waals
	764P	PHE	Van Der Waals
	766P	PRO	Van Der Waals
	765P	ALE	Van Der Waals
	804P	PHE	Van Der Waals
	681P	GLU	Van Der Waals
	748P	ALA	Van Der Waals
	805P	LEU	Van Der Waals
	801P	PRO	Van Der Waals
Ganoderic acid C1 CID-471004	802P	GLN	Van Der Waals
	681P	GLU	Conventional Hydrogen bond
	748P	ALA	Van Der Waals
	683P	GLY	Van Der Waals
	752P	ARG	Van Der Waals
	804P	PHE	Van Der Waals
	751P	TRP	Van Der Waals
	755P	THR	Van Der Waals
	801P	PRO	Van Der Waals
	802P	GLN	Van Der Waals
	678P	GLU	Van Der Waals
	805P	LEU	Van Der Waals
	808P	LYS	Van Der Waals
Ganoderic acid M CID-5317490	648P	VAL	Alkyl
	685P	VAL	Alkyl
	682P	PRO	Alkyl
	808P	LYS	Conventional Hydrogen bond
	752P	ARG	Conventional Hydrogen bond
	751P	TRP	Conventional Hydrogen bond
	678P	GLU	Van Der Waals
	805P	LEU	Van Der Waals
	681P	GLU	Van Der Waals
	683P	GLY	Van Der Waals
	748P	ALA	Van Der Waals
	714P	HSD	Van Der Waals
	715P	VAL	Van Der Waals
Ganoderic acid I CID-10075137	711P	GLN	Van Der Waals
	755P	THR	Van Der Waals
	804P	PHE	Van Der Waals
	801P	PRO	Van Der Waals
	802P	GLN	Van Der Waals
	684P	VAL	Alkyl
	685P	VAL	Alkyl
	682P	PRO	Alkyl
	752P	ARG	Conventional Hydrogen bond
	681P	GLU	Conventional Hydrogen bond
	678P	GLU	Conventional Hydrogen bond
	802P	GLN	Conventional Hydrogen bond
	808P	LYS	Conventional Hydrogen bond
Standard CID-2800	682P	PRO	Alkyl
	685P	VAL	Alkyl
	801P	PRO	Alkyl
	751P	TRP	Alkyl
	748P	ALA	Alkyl
	752P	ARG	Alkyl
	805P	LEU	Alkyl
	681P	GLU	Pi-Anion

3.4. Physicochemical properties and pharmacokinetic properties prediction analysis.

A substance's bioactivity is mostly determined by its absorption, distribution, metabolism, and excretion (ADME) properties, which are all linked to its pharmacokinetic properties. The dietary bioavailability of phytochemicals to target cells and their absorption and metabolism in the human body are all important factors in increasing bioactivity and

preserving bodily health [57]. Phytochemicals/test substances must break hydrogen bonds in the aqueous environment and partition across the membrane in order to permeate the membrane [58]. The hydrogen-bonding potential of a chemical is linked to its polar surface area (PSA), whereas membrane permeability is linked to molecular mass and lipophilicity [59]. As a result, in order to pass the standard clinical studies required to be considered as a prospective therapeutic candidate, the ADME properties must be assessed earlier in the drug design and discovery process [60]. The physicochemical properties and ADMET of the selected GAs and standard drugs were assessed using the pkCSM database (<http://biosig.unimelb.edu.au>). The physicochemical properties of the selected components are listed in Table 4. GAs violates Lipinski's rule of 5 due to their increased molecular weight (CID-471002 molecular weight-516.675, CID-74036828 molecular weight-574.711, CID-471004 molecular weight-514.659, CID-5317490 molecular weight-530.658, CID-10075137 molecular weight-532.974), while the standard drug violated violates the Lipinski's rule of 5 due to its increased octanol-water partition coefficient (CID-2800 logP-6.5626). The polar surface area of selected compounds was (CID-471002) 219.683, (CID-74036828) 241.643, (CID-471004) 219.006, (CID-5317490) 223.800, (CID-10075137) 224.433 and (CID-2800) 178.952.

Table 4. Molecular properties of GAs and standard.

SL.NO	Compound Name	Molecular Weight	Log P	Rotatable Bonds	Acceptors	Donors	Surface Area
1	Ganoderic Acid A	516.675	4.1315	6	6	3	219.638
2	Ganoderic Acid K	574.711	3.6731	7	8	3	241.643
3	Ganoderic Acid C1	514.659	4.3397	6	6	2	219.006
4	Ganoderic Acid M	530.658	3.3105	6	7	3	223.800
5	Ganoderic Acid I	532.674	3.2464	6	7	4	224.433
6	Standard	405.969	6.5626	9	2	0	178.952

The predicted absorption properties of the selected components are listed in Table 5. According to the obtained results, the water solubility of GAs was higher as compared to standard (CID-471002 -3.984log mol/L, CID-74036828 -4.068log mol/L, CID-471004 -3.801log mol/L, CID-5317490 -3.768log mol/L, and CID-10075137 -3.567log mol/L) as compared to standard (CID-2800 -6.682log mol/L). However, the Caco2 permeability of GAs was observed to be lower as compared to the standard. The selected components showed a good percentage of intestinal absorption (CID-471002 64.393%, CID-74036828 64.903%, CID-471004 70.11%, CID-5317490 62.157%, CID-10075137 56.371% and CID-2800 94.919) and skin permeability. Both GAs and standard were likely to be substrates of P-glycoprotein substrate. GAs modulated P-glycoprotein 1-mediated transport, whereas the standard drug inhibited P-glycoprotein 1-mediated transport.

Table 5. Predicted absorption properties GAs and standard.

SL. No	Compound Name	Water Solubility (log mol/L)	Caco2 Permeability (log p app in 10 ⁻⁶ cm/s)	Intestinal absorption (human) (%) absorbed)	Skin Permeability (log Kp)	P-glycoprotein Substrate (Yes/No)	P-glycoprotein 1 Inhibitor (Yes/No)	P-glycoprotein 2 Inhibitor (Yes/No)
1	Ganoderic Acid A	-3.984	0.608	64.393	-2.737	Yes	No	Yes
2	Ganoderic Acid K	-4.068	-0.059	64.903	-2.736	Yes	No	Yes
3	Ganoderic Acid C1	-3.801	0.681	70.111	-2.736	Yes	No	Yes
4	Ganoderic Acid M	-3.768	-0.037	62.157	-2.736	Yes	No	Yes

SL. No	Compound Name	Water Solubility (log mol/L)	Caco2 Permeability (log p app in 10 ⁻⁶ cm/s)	Intestinal absorption (human) (% absorbed)	Skin Permeability (log Kp)	P-glycoprotein Substrate (Yes/No)	P-glycoprotein 1 Inhibitor (Yes/No)	P-glycoprotein 2 Inhibitor (Yes/No)
5	Ganoderic Acid I	-3.567	-0.081	56.371	-2.735	Yes	No	No
6	Standard	-6.682	0.938	94.919	-2.734	Yes	Yes	Yes

The predicted distribution properties of the selected components are listed in Table 6. The steady-state volume of distribution (VD_{ss}) was found to be low for all the components, including the standard (CID-471002, -0.599log L/Kg; CID-74036828, -0.589log L/Kg; CID-471004, -0.527log L/Kg; CID-5317490, -0.542log L/Kg; CID-10075137, -0.78log L/Kg and CID-2800, 0.66log L/Kg). The fraction unbound of GAs was observed to be more (CID-471002, 0.182Fu; CID-74036828, 0.207 Fu; CID-471004, 0.197Fu; CID-5317490, 0.238Fu; CID-10075137, 0.273Fu) compared to the standard drug (CID-2800, 0.141Fu). GAs was observed to have low to moderate BBB and CNS permeability due to their increased molecular weight.

Table 6. Predicted distribution properties of GAs and standard.

SL.NO	Compound Name	VD _{ss} (human) (log L/kg)	Fraction Unbound (human) (Fu)	BBB Permeability (log BB)	CNS Permeability (log PS)
1	Ganoderic Acid A	-0.599	0.182	-0.911	-3
2	Ganoderic Acid K	-0.589	0.207	-1.239	-3.06
3	Ganoderic Acid C1	-0.527	0.197	-0.645	-2.923
4	Ganoderic Acid M	-0.542	0.238	-0.997	-3.026
5	Ganoderic Acid I	-0.78	0.273	-0.922	-3.089
6	Standard	0.66	0.141	1.213	-1371

The predicted metabolism properties of GAs and standard are listed in Table 7. Both GAs and standard drug were observed as not likely to be metabolized by CYP2D6. However, GAA, GAK, and GAC1 were likely to be metabolized by CYP3A4. GAM and GAI were observed to be not metabolized by CYP3A4. GAs was observed not to inhibit any of the CYP450s compared to the standard drug that inhibited all CYP450s except for CYP2C9.

Table 7. Predicted metabolism properties of GAs and standard.

SL. NO	Compound Name	CYP2D6 Substrate (Yes/No)	CYP3A4 Substrate (Yes/No)	CYP1A2 Inhibitor (Yes/No)	CYP2C19 Inhibitor (Yes/No)	CYP2C9 Inhibitor (Yes/No)	CYP2D6 Inhibitor (Yes/No)	CYP3A4 Inhibitor (Yes/No)
1	Ganoderic Acid A	No	Yes	No	No	No	No	No
2	Ganoderic Acid K	No	Yes	No	No	No	No	No
3	Ganoderic Acid C1	No	Yes	No	No	No	No	No
4	Ganoderic Acid M	No	No	No	No	No	No	No
5	Ganoderic Acid I	No	No	No	No	No	No	No
6	Standard	No	Yes	Yes	Yes	No	Yes	Yes

The predicted excretion properties of GAs and standard drug are listed in Table 8. The total clearance of the selected components was CID-471002, 0.242 log ml/min/kg; CID-74036828, 0.209 log ml/min/kg; CID-471004, 0.185 log ml/min/kg; CID-5317490, 0.263 log ml/min/kg; CID-10075137, 0.236 log ml/min/kg respectively and the total clearance of standard drug was CID-2800, 0.533 log ml/min/kg. Neither GAs nor the standard drug was observed to be renal OCT2 substrates.

Table 8. Predicted excretion properties of GAs and standard.

SL.NO	Compound Name	Total Clearance (log ml/min/kg)	Renal OCT2 Substrate (Yes/No)
1	Ganoderic Acid A	0.242	No
2	Ganoderic Acid K	0.209	No
3	Ganoderic Acid C1	0.185	No
4	Ganoderic Acid M	0.263	No
5	Ganoderic Acid I	0.236	No
6	Standard	0.553	No

The predicted toxicity properties of the selected components are listed in Table 9. GA's were observed to be AMES negative and hence non-mutagenic, whereas the standard drug was observed to be AMES positive and hence mutagenic. The maximum tolerated dose of GA's was CID-471002, 0.147 log mg/kg/day; CID-74036828, 0.32 log mg/kg/day; CID-471004, 0.376 log mg/kg/day; CID-5317490, 0.261 log mg/kg/day; CID-10075137, 0.642 log mg/kg/day respectively and the maximum tolerated dose of the standard drug was 0.46 log mg/kg/day, both GA's and the standard drug showed a low range of maximum tolerated dose. GA's were predicted to neither inhibit hERG1 nor hERG2 as compared to the standard, which was predicted not to inhibit hERG1 but likely to inhibit hERG2. The oral rat acute toxicity (LD50) of GAs was observed to be CID-471002, 2.622 mol/kg; CID-74036828, 2.812 mol/kg; CID-471004, 2.725 mol/kg; CID-5317490, 2.784 mol/kg; CID-10075137, 2.863 mol/kg respectively and the oral rat acute toxicity (LD50) of the standard drug was observed to be CID-2800, 2.309 mol/kg. GAs showed negative results for hepatotoxicity, and standard showed positive results for hepatotoxicity. Thus, GAs are not associated with disrupted normal liver function. The minnow toxicity values of GAs were CID-471002, 1.645 log mM; CID-74036828, 3.45 log mM; CID-471004, 1.581 log mM; CID-5317490, 2.796 log mM; CID-10075137, 2.833 log mM respectively indicating non-toxicity and the minnow toxicity value of the standard drug was 0.37 log mM indicating toxicity. The selected components of *Ganoderma lucidum* showed better ADME properties as compared to standard drugs without any major toxicity.

Table 9. Predicted toxicity parameters of GAs and standard.

Sl. no	Comp. Name	AMES Toxicity Yes/No	Maximum Tolerated Dose (human)(log mg/kg/day)	hERG-1 Inhibitor Yes/No	hERG-2 Inhibitor Yes/No	Oral Rat Acute Toxicity (LD50) (mol/kg)	Oral Rat Chronic Toxicity (log mg/kg_bw/day)	Hepato-toxicity (Yes/No)	Skin Sensitisation (Yes/No)	<i>T.pyriformis</i> Toxicity (log ug/L)	Minnow Toxicity (log Mm)
1	Ganoderic Acid A	No	0.147	No	No	2.622	1.85	No	No	0.285	1.645
2	Ganoderic Acid K	No	0.32	No	No	2.812	2.012	No	No	0.285	3.45
3	Ganoderic Acid C1	No	0.376	No	No	2.725	1.507	No	No	0.285	1.581
4	Ganoderic Acid M	No	0.261	No	No	2.784	1.966	No	No	0.285	2.796
5	Ganoderic Acid I	No	0.642	No	No	2.863	1.985	No	No	0.285	2.833
6	Standard	Yes	0.46	No	Yes	2.309	-0.104	Yes	No	0.297	0.37

3.5. Molecular dynamics simulation.

Though a widespread and successful application, protein-ligand docking only gives the static view of the binding pose of the ligand with the active site of the receptor identical to a photographic image. Molecular dynamics (MD) should be utilized to simulate the atoms of

particles in the framework as a time component with the incorporation of Newton's situations of movements [61-63]. Ganoderic acid A was selected for dynamic molecular studies with maximum binding capacity with 1E3G, and better pharmacokinetic predicted parameters than standard. Molecular dynamic simulation for 100 ns was carried out for GAA- 1E3G complex and the unbound form of the 1E3G target protein, and the respective results were interpreted. Molecular dynamic trajectories analysis was performed using root mean square deviation (RMSD) and root mean square fluctuation (RMSF) of receptor atoms, to interpret the fluctuations and stability of the protein-ligand complex.

RMSD is a significant parameter in investigating the equilibration of molecular dynamics trajectories and checking the stability of the protein-ligand complex system during simulation. RMSD of the protein backbone atoms was plotted against time to assess the structural conformation variations. Initially, the GAA-1E3G complex showed variations in backbone RMSD till 20 ns ranging from 0.6 to 1.8nm. The stable conformation was attained between the time period 21ns and 85ns with no considerable deviations. The complex again showed variations at the final stage, from 86ns to 100ns. The RMSD of the GAA- 1E3G complex is depicted in Figure 7.

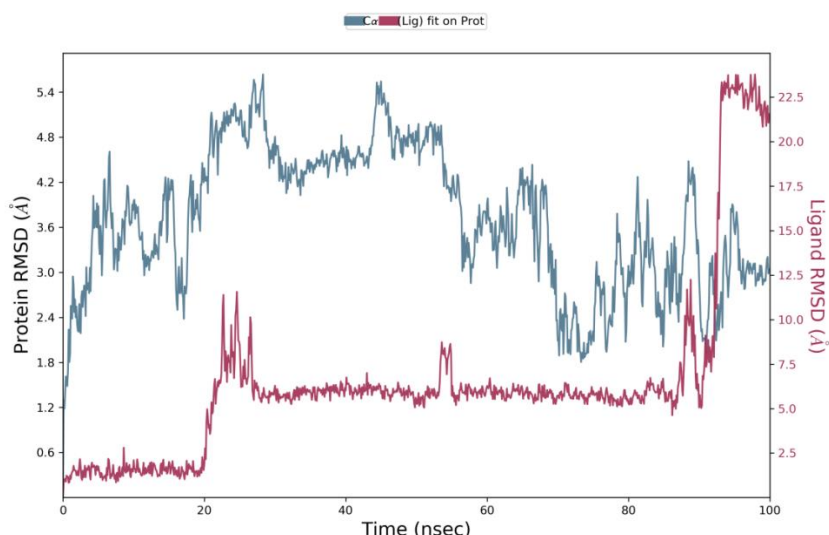


Figure 7. RMSD study plot of 1E3G-GAA for 100 ns molecular dynamic simulation.

RMSF is another significant parameter in investigating the stability and flexibility of protein-ligand complex systems during simulation [64]. Changes in the behavior of target protein amino acid residues after binding with a ligand were analyzed using RMSF [65,66]. The RMSF values for C α atoms of the protein were calculated and plotted with respect to the residues. In the examined GAA-1E3G complex, the amino acid residues showed no fluctuations for the entire simulation, and the resulting graph was observed to be smooth. The amino acids of 1E3G, which interacted with GAA in molecular docking, also showed low fluctuation values during molecular dynamic simulation viz. GLN783 and GLU872. The obtained results revealed that the binding of the ligand did not stimulate any major effects on the flexibility of the protein, as depicted in Figure 8.

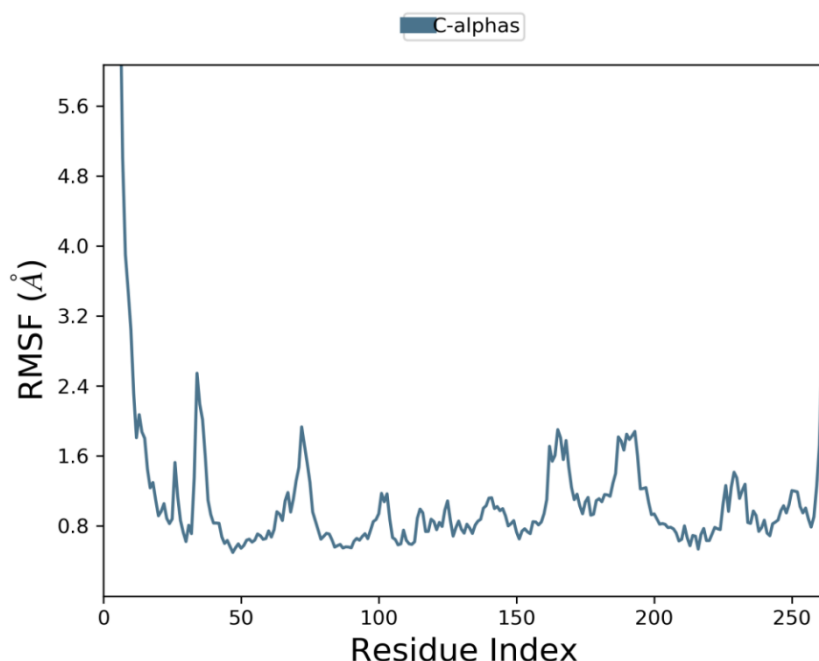


Figure 8. RMSF study plot of 1E3G-GAA for 100 ns molecular dynamic simulation.

Protein interactions with the ligand were monitored throughout the simulation. The ligand showed a 0.97 interaction fraction with amino acid residue GLN783 through hydrogen bonding with ligand-mediated by a water molecule, suggesting that, 97% of the simulation time, the interaction was maintained. Similarly, the ligand showed an interaction fraction of 0.73 with GLU872, 0.44 with ARG779, 0.4 with SER782, 0.3 with GLN875, 0.18 with LYS883, and 0.1 with SER778, respectively, as depicted in Figure 9. A schematic of detailed ligand atom interactions with the protein residues is depicted in Figure 10. The ligand interaction with GLU872 occurred for 64% of the simulation time in the selected trajectory, and the ligand interactions with GLN783 occurred for 52% of the simulation time in the selected trajectory.

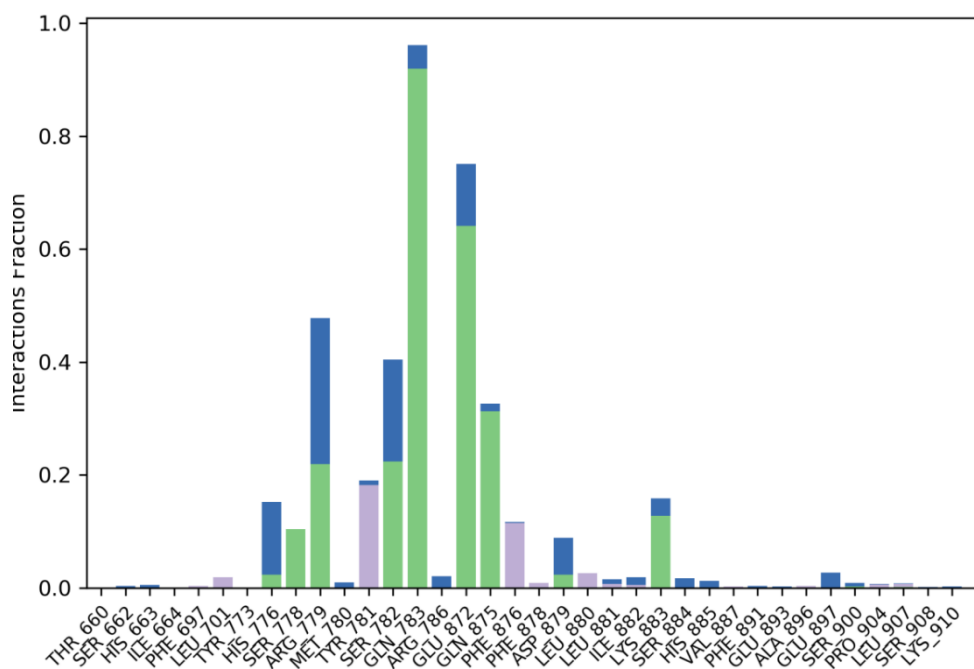


Figure 9. Amino acid residues of protein interactions with the ligand.

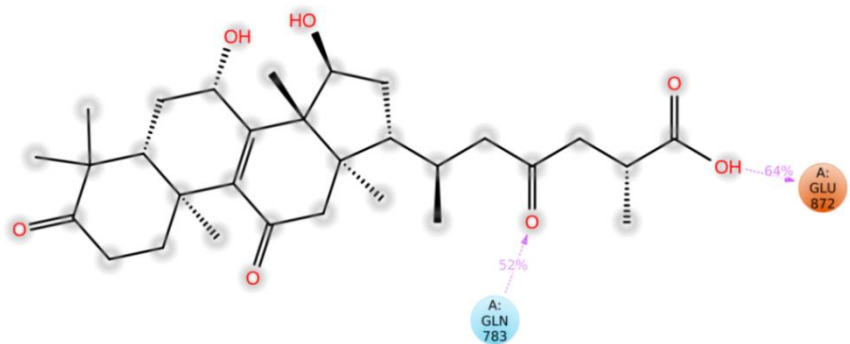


Figure 10. Ligand protein contacts.

4. Conclusions

Ganoderic acid A has a wide range of pharmacological activities like antioxidant, anti-cancer, anti-diabetic, anti-inflammatory, anti-hyperlipidemic, anti-cyst, immunomodulatory, anti-tumor, and antiandrogenic. PCOS is characterized by endocrinological, gynecological, and metabolic abnormalities and needs a treatment consisting of a broad pharmacological approach. In women with hyperandrogenic PCOS, serum levels of testosterone (T), the pro-androgens androstenedione (A4) and DHEA, as well as the enzyme required to convert pro-androgens to bioactive androgens, 3-hydroxysteroid dehydrogenase (3-HSD), are all increased. Androgen receptor (AR) is linked to the PCOS phenotype and may also be involved in folliculogenesis. In this study, we explored the action of ganoderic acids in treating PCOS by inhibiting androgen receptors and thus decreasing the androgen levels. The antiandrogenic potential of ganoderic acids has been proven in this study by conducting a detailed pharmacoinformatics- based molecular docking study of GAs against androgen receptors. *In silico* molecular docking, investigations revealed that five of the GAs (GAA, GAK, GAC1, GAM, and GAI) had inhibitory action on 1E3G. Molecular dynamic simulation experiments and *in silico* pharmacokinetic prediction analyses also reveal the safety profile of Ganoderic Acid A and the stability of the protein–ligand complex. To determine the effectiveness of GAA in treating PCOS, computational studies on other receptors involved in PCOS can be carried out. It is also necessary to conduct *in vivo* and *in vitro* research to explore the pharmacological activities.

Funding

This research received no external funding.

Acknowledgments

The authors thank the Department of Pharmaceutical Chemistry, Faculty of Pharmacy, M. S. Ramaiah University of Applied, Bengaluru, for providing a computational facility.

Conflicts of Interest

The authors declare no conflict of interest.

References

1. Eissa, M. Polycystic ovarian syndrome (PCOS) this mysterious disease. *MOJ Womens Health* **2017**, *4*, 40-43, <https://doi.org/10.15406/mojwh.2017.04.00082>.

2. Pachiappan, S.; Ramalingam, K.; Balasubramanian, A. A review on phytomedicine and their mechanism of action on PCOS. *Int. J. Cur. Res. Rev* **2020**, *12*, 81.
3. Brady, C.; Mousa, S.S.; Mousa, S.A. Polycystic ovary syndrome and its impact on women's quality of life: More than just an endocrine disorder. *Drug, healthcare and patient safety* **2009**, *1*, 9, <https://doi.org/10.2147/dhps.s4388>.
4. Prajapati, D.P.; Patel, M.; Dharamsi, A. Beneficial effect of polyherbal formulation in letrozole induced polycystic ovarian syndrome (PCOS). *Journal of Traditional and Complementary Medicine* **2022**, <https://doi.org/10.1016/j.jtcme.2022.08.003>.
5. Bharathi, R.V.; Swetha, S.; Neerajaa, J.; Madhavica, J.V.; Janani, D.M.; Rekha, S.; Ramya, S.; Usha, B. An epidemiological survey: Effect of predisposing factors for PCOS in Indian urban and rural population. *Middle East Fertility Society Journal* **2017**, *22*, 313-316, <https://doi.org/10.1016/j.mefs.2017.05.007>.
6. Gupta, M.; Singh, D.; Toppo, M.; Priya, A.; Sethia, S.; Gupta, P. A cross sectional study of polycystic ovarian syndrome among young women in Bhopal, Central India. *Int J Community Med Public Health* **2018**, *5*, 95-100.
7. Liu, J.; Wu, Q.; Hao, Y.; Jiao, M.; Wang, X.; Jiang, S.; Han, L. Measuring the global disease burden of polycystic ovary syndrome in 194 countries: Global Burden of Disease Study 2017. *Human Reproduction* **2021**, *36*, 1108-1119, <https://doi.org/10.1093/humrep/deaa371>.
8. Nidhi, R.; Padmalatha, V.; Nagarathna, R.; Amritanshu, R. Prevalence of polycystic ovarian syndrome in Indian adolescents. *Journal of pediatric and adolescent gynecology* **2011**, *24*, 223-227, <https://doi.org/10.1016/j.jpag.2011.03.002>.
9. Rao, S.; Budh, N.; Abdul Salam, A.A.; Mohammed, C.A.; Jain, A.; Sethuraman, A.R.; Singh, M.M. Effectiveness of Model based Training on Self-Breast Examination among Reproductive Age Group Women in the Community. *Indian Journal of Public Health Research & Development* **2021**, *12*, <https://doi.org/10.37506/ijphrd.v12i4.16570>.
10. Stener-Victorin, E.; Padmanabhan, V.; Walters, K.A.; Campbell, R.E.; Benrick, A.; Giacobini, P.; Dumesic, D.A.; Abbott, D.H. Animal models to understand the etiology and pathophysiology of polycystic ovary syndrome. *Endocrine reviews* **2020**, *41*, bnaa010, <https://doi.org/10.1210/endrev/bnaa010>.
11. Goodarzi, M.O.; Dumesic, D.A.; Chazenbalk, G.; Azziz, R. Polycystic ovary syndrome: etiology, pathogenesis and diagnosis. *Nature reviews endocrinology* **2011**, *7*, 219-231, <https://doi.org/10.1038/nrendo.2010.217>.
12. Glueck, C.J.; Goldenberg, N. Characteristics of obesity in polycystic ovary syndrome: etiology, treatment, and genetics. *Metabolism* **2019**, *92*, 108-120, <https://doi.org/10.1016/j.metabol.2018.11.002>.
13. Cooney, L.G.; Dokras, A. Depression and anxiety in polycystic ovary syndrome: etiology and treatment. *Current psychiatry reports* **2017**, *19*, 1-10, <https://doi.org/10.1007/s11920-017-0834-2>.
14. Matalliotakis, I.; Kourtis, A.; Koukoura, O.; Panidis, D. Polycystic ovary syndrome: etiology and pathogenesis. *Archives of gynecology and obstetrics* **2006**, *274*, 187-197, <https://link.springer.com/article/10.1007/s00404-006-0171-x>.
15. Taghadomi Masoumi, Z.; Eshraghian, M.R.; Hedayati, M.; Pishva, H. Association between uncoupling protein 2, adiponectin and resting energy expenditure in obese women with normal and low resting energy expenditure. *Gynecological Endocrinology* **2018**, *34*, 166-170, <https://doi.org/10.1080/09513590.2017.1379492>.
16. Maqbool, M.; Dar, M.A.; Gani, I.; Geer, M.I. Insulin resistance and polycystic ovary syndrome: a review. *Journal of drug delivery and therapeutics* **2019**, *9*, 433-436, <https://doi.org/10.22270/jddt.v9i1-s.2275>.
17. Kalugina, A.; Bobrov, K.Y. Polycystic ovary syndrome: modern view and it's role in infertility (a review). *Problemy reproduktsii* **2015**, *2*, 31-35, <http://dx.doi.org/10.17116/repro201521231-35>.
18. Simic, D.; Nikolic Turnic, T.; Dimitrijevic, A.; Zivadinovic, A.; Milosevic-Stevanovic, J.; Djuric, D.; Zivkovic, V.; Jakovljevic, V. Potential role of d-chiro-inositol in reducing oxidative stress in the blood of nonobese women with polycystic ovary syndrome. *Canadian journal of physiology and pharmacology* **2022**, *100*, 629-636, <https://doi.org/10.1139/cjpp-2021-0766>.
19. Murri, M.; Insenser, M.; Escobar-Morreale, H.F. Metabolomics in polycystic ovary syndrome. *Clinica chimica acta* **2014**, *429*, 181-188, <https://doi.org/10.1016/j.cca.2013.12.018>.
20. Jin, P.; Xie, Y. Treatment strategies for women with polycystic ovary syndrome. *Gynecological Endocrinology* **2018**, *34*, 272-277, <https://doi.org/10.1080/09513590.2017.1395841>.

21. Debras, E.; Fernandez, H.; Neveu, M.; Deffieux, X.; Capmas, P. Ovarian drilling in polycystic ovary syndrome: Long term pregnancy rate. *European Journal of Obstetrics & Gynecology and Reproductive Biology: X* **2019**, *4*, 100093, <https://doi.org/10.1016/j.eurox.2019.100093>.
22. Malik, S.M.; Traub, M.L. Defining the role of bariatric surgery in polycystic ovarian syndrome patients. *World Journal of Diabetes* **2012**, *3*, 71, <https://doi.org/10.4239%2Fwj.d.v3.i4.71>.
23. Moini Jazani, A.; Nasimi Doost Azgomi H.; Nasimi Doost Azgomi A.; Nasimi Doost Azgomi R. A comprehensive review of clinical studies with herbal medicine on polycystic ovary syndrome (PCOS). *J Pharm Sci* **2019**, *27*, 863-877, <https://doi.org/10.1007/s40199-019-00312-0>.
24. ita Wal, A.; Wal, P.; ita Saraswat, N.; Wadhwa, S. A Detailed Review on Herbal Treatments for Treatment of PCOS-Polycystic ovary syndrome (PCOS). *Current Nutraceuticals* **2021**, *2*, 192-202, <https://doi.org/10.2174/2665978602666210805092103>.
25. Arentz, S.; Abbott, J.; Smith, C. Bensoussan AJBc, medicine a. Herbal medicine for the management of polycystic ovary syndrome (PCOS) and associated oligo/amenorrhoea and hyperandrogenism; a review of the laboratory evidence for effects with corroborative clinical findings. *BMC Complement Altern Med* **2014**, *14*, 511, <https://doi.org/10.1186/1472-6882-14-511>.
26. Andhalkar, S.; Chaware, V.; Redasani, V. A review on medicinal plants of natural origin for treatment of polycystic ovarian syndrome (PCOS). *Asian Journal of Pharmaceutical Research and Development* **2021**, *9*, 76-81, <https://doi.org/10.22270/ajprd.v9i3.949>.
27. Abasian, Z.; Rostamzadeh, A.; Mohammadi, M.; Hosseini, M.; Rafieian-Kopaei, M. A review on role of medicinal plants in polycystic ovarian syndrome: pathophysiology, neuroendocrine signaling, therapeutic status and future prospects. *Middle East Fertility Society Journal* **2018**, *23*, 255-262, <https://doi.org/10.1016/j.mefs.2018.04.005>.
28. Sanodiya, B.S.; Thakur, G.S.; Baghel, R.K.; Prasad, G.; Bisen, P. *Ganoderma lucidum*: a potent pharmacological macrofungus. *Current pharmaceutical biotechnology* **2009**, *10*, 717-742, <https://doi.org/10.2174/138920109789978757>.
29. Ahmad, M.F. *Ganoderma lucidum*: Persuasive biologically active constituents and their health endorsement. *Biomedicine & Pharmacotherapy* **2018**, *107*, 507-519, <https://doi.org/10.1016/j.biopha.2018.08.036>.
30. Ren, L. Protective effect of ganoderic acid against the streptozotocin induced diabetes, inflammation, hyperlipidemia and microbiota imbalance in diabetic rats. *Saudi Journal of Biological Sciences* **2019**, *26*, 1961-1972, <https://doi.org/10.1016/j.sjbs.2019.07.005>.
31. Huang, C.-H.; Lin, W.-K.; Chang, S.H.; Tsai, G.-J. Evaluation of the hypoglycaemic and antioxidant effects of submerged *Ganoderma lucidum* cultures in type 2 diabetic rats. *Mycology* **2021**, *12*, 82-93, <https://doi.org/10.1080/21501203.2020.1733119>.
32. Cho, J.Y.; Sadiq, N.B.; Kim, J.-C.; Lee, B.; Hamayun, M.; Lee, T.S.; Kim, H.S.; Park, S.H.; Nho, C.W.; Kim, H.-Y. Optimization of antioxidant, anti-diabetic, and anti-inflammatory activities and ganoderic acid content of differentially dried *Ganoderma lucidum* using response surface methodology. *Food Chemistry* **2021**, *335*, 127645, <https://doi.org/10.1016/j.foodchem.2020.127645>.
33. Zhu, J.; Jin, J.; Ding, J.; Li, S.; Cen, P.; Wang, K.; Wang, H.; Xia, J. Ganoderic Acid A improves high fat diet-induced obesity, lipid accumulation and insulin sensitivity through regulating SREBP pathway. *Chemico-Biological Interactions* **2018**, *290*, 77-87, <https://doi.org/10.1016/j.cbi.2018.05.014>.
34. Meng, J.; Wang, S.-z.; He, J.-z.; Zhu, S.; Huang, B.-y.; Wang, S.-y.; Li, M.; Zhou, H.; Lin, S.-q.; Yang, B.-x. Ganoderic acid A is the effective ingredient of *Ganoderma* triterpenes in retarding renal cyst development in polycystic kidney disease. *Acta Pharmacologica Sinica* **2020**, *41*, 782-790, <https://www.nature.com/articles/s41401-019-0329-2>.
35. Liu, R.-M.; Li, Y.-B.; Zhong, J.-J. Cytotoxic and pro-apoptotic effects of novel ganoderic acid derivatives on human cervical cancer cells *in vitro*. *European journal of pharmacology* **2012**, *681*, 23-33, <https://doi.org/10.1016/j.ejphar.2012.02.007>.
36. Gill, B.S.; Kumar, S. Evaluating antioxidant potential of ganoderic acid A in STAT 3 pathway in prostate cancer. *Molecular biology reports* **2016**, *43*, 1411-1422, <https://doi.org/10.1007/s11033-016-4074-z>.
37. Gomeni, R.; Bani, M.; D'Angeli, C.; Corsi, M.; Bye, A. Computer-assisted drug development (CADD): an emerging technology for designing first-time-in-man and proof-of-concept studies from preclinical experiments. *European journal of pharmaceutical sciences* **2001**, *13*, 261-270, [https://doi.org/10.1016/s0928-0987\(01\)00111-7](https://doi.org/10.1016/s0928-0987(01)00111-7).

38. Frye, L.; Bhat, S.; Akinsanya, K.; Abel, R. From computer-aided drug discovery to computer-driven drug discovery. *Drug Discovery Today: Technologies* **2021**, *39*, 111-117, <https://doi.org/10.1016/j.ddtec.2021.08.001>.
39. LA, S.V.N.T.J.; Maguire, G.; Govender, T.; Naicker, T.; Kruger, H.G. Current trends in computer aided drug design and a highlight of drugs discovered via computational techniques: A review. *Eur. J. Med. Chem* **2021**, *224*, 113705, <https://doi.org/10.1016/j.ejmech.2021.113705>.
40. Usha, T.; Shanmugarajan, D.; Goyal, A.K.; Kumar, C.S.; Middha, S.K. Recent updates on computer-aided drug discovery: time for a paradigm shift. *Current topics in medicinal chemistry* **2017**, *17*, 3296-3307, <https://doi.org/10.2174/1568026618666180101163651>.
41. Feng, H.B.J.W.Z.; Weissig, G.G.T.B.H. IN Shindyalov PE Bourne . *Nucleic Acids Res* **2000**, *28*, 235-242, <https://doi.org/10.1093/nar/28.1.235>.
42. Yang, Y.; Zhang, H.; Zuo, J. Advances in research on the active constituents and physiological effects of *Ganoderma lucidum*. *Biomed dermatol* **2019**, <https://biomeddermatol.biomedcentral.com/articles/10.1186/s41702-019-0044-0>.
43. Mohanraj, K.; Karthikeyan, B.S.; Vivek-Ananth, R.; Chand, R.; Aparna, S.; Mangalapandi, P.; Samal, A. IMPPAT: a curated database of Indian medicinal plants, phytochemistry and therapeutics. *Scientific reports* **2018**, *8*, 1-17, <https://www.nature.com/articles/s41598-018-22631-z>.
44. Fradera, X.; Babaoglu, K. Overview of methods and strategies for conducting virtual small molecule screening. *Current protocols in chemical biology* **2017**, *9*, 196-212, <https://doi.org/10.1002/cpch.27>.
45. Gaillard, T. Evaluation of AutoDock and AutoDock Vina on the CASF-2013 benchmark. *Journal of chemical information and modeling* **2018**, *58*, 1697-1706, <https://doi.org/10.1021/acs.jcim.8b00312>.
46. Mohan, U.P.; Kunjiappan, S.; Tirupathi Pichiah, P.; Arunachalam, S. Adriamycin inhibits glycolysis through downregulation of key enzymes in *Saccharomyces cerevisiae*. *3 Biotech* **2021**, *11*, 1-13, <https://link.springer.com/article/10.1007/s13205-020-02530-9>.
47. Jia, C.-Y.; Li, J.-Y.; Hao, G.-F.; Yang, G.-F. A drug-likeness toolbox facilitates ADMET study in drug discovery. *Drug Discovery Today* **2020**, *25*, 248-258, <https://doi.org/10.1016/j.drudis.2019.10.014>.
48. Kalimuthu, A.K.; Panneerselvam, T.; Pavadai, P.; Pandian, S.R.K.; Sundar, K.; Murugesan, S.; Ammunje, D.N.; Kumar, S.; Arunachalam, S.; Kunjiappan, S. Pharmacoinformatics-based investigation of bioactive compounds of Rasam (South Indian recipe) against human cancer. *Scientific reports* **2021**, *11*, 1-19, <https://www.nature.com/articles/s41598-021-01008-9>.
49. Kunjiappan, S.; Sankaranarayanan, M.; Kumar, B.K.; Pavadai, P.; Babkiewicz, E.; Maszczyk, P.; Glodkowska-Mrowka, E.; Arunachalam, S.; Pandian, S.R.K.; Ravishankar, V. Capsaicin-loaded solid lipid nanoparticles: Design, biodistribution, *in silico* modeling and *in vitro* cytotoxicity evaluation. *Nanotechnology* **2020**, *32*, 095101, <https://doi.org/10.1088/1361-6528/abc57e>.
50. Jorgensen, W.; Chandrasekhar, J.; Madura, J. Impey, RW; Klein, ML. Comparison of simple potential functions for simulating liquid water. *J. Chem. Phys* **1983**, *79*, 926, <https://doi.org/10.1063/1.445869>,
51. Hu, Y.; Sinnott, S.B. Constant temperature molecular dynamics simulations of energetic particle–solid collisions: comparison of temperature control methods. *Journal of Computational Physics* **2004**, *200*, 251-266, <https://doi.org/10.1016/j.jcp.2004.03.019>.
52. Chen, S.; Feng, J.; Zhao, C.; Wang, L.; Meng, L.; Liu, C.; Cai, S.; Jia, Y.; Qu, L.; Shou, C. Aiphanol, a native compound, suppresses angiogenesis via dual-targeting VEGFR2 and COX2. *Signal transduction and targeted therapy* **2021**, *6*, 1-3, <https://www.nature.com/articles/s41392-021-00739-5>.
53. Alamri, M.A. Pharmacoinformatics and molecular dynamic simulation studies to identify potential small-molecule inhibitors of WNK-SPAK/OSR1 signaling that mimic the RFQV motifs of WNK kinases. *Arabian Journal of Chemistry* **2020**, *13*, 5107-5117, <https://doi.org/10.1016/j.arabjc.2020.02.010>.
54. Shah, N.A.; Antoine, H.J.; Pall, M.; Taylor, K.D.; Azziz, R.; Goodarzi, M.O. Association of androgen receptor CAG repeat polymorphism and polycystic ovary syndrome. *The Journal of Clinical Endocrinology & Metabolism* **2008**, *93*, 1939-1945, <https://doi.org/10.1210/jc.2008-0038>.
55. Rodriguez Paris, V.; Bertoldo, M.J. The mechanism of androgen actions in PCOS etiology. *Medical sciences* **2019**, *7*, 89, <https://doi.org/10.3390/medsci7090089>.
56. Gupte, A.; Palande, A.; Venkata, S.; Pol, R. Docking studies of *Ganoderma lucidum*. *International Journal of Pharmaceutical Sciences and Research* **2018**, *9*, https://www.researchgate.net/profile/Reshma-Pol/publication/323846488_Docking_studies_on_Ganoderma_lucidum/links/5ab0933d0f7e9b4897c1e16f/Docking-studies-on-Ganoderma-lucidum.pdf.

57. da Silva, B.V.; Barreira, J.C.; Oliveira, M.B.P. Natural phytochemicals and probiotics as bioactive ingredients for functional foods: Extraction, biochemistry and protected-delivery technologies. *Trends in Food Science & Technology* **2016**, *50*, 144-158, <https://doi.org/10.1016/j.tifs.2015.12.007>.
58. Cohen, J. *Statistical power analysis for the behavioral sciences*; Routledge: 2013, <https://www.taylorfrancis.com/books/mono/10.4324/9780203771587/statistical-power-analysis-behavioral-sciences-jacob-cohen>.
59. Alex, A.; Millan, D.S.; Perez, M.; Wakenhut, F.; Whitlock, G.A. Intramolecular hydrogen bonding to improve membrane permeability and absorption in beyond rule of five chemical space. *MedChemComm* **2011**, *2*, 669-674, <https://pubs.rsc.org/en/content/articlelanding/2011/md/c1md00093d>.
60. Hughes, J.P.; Rees, S.; Kalindjian, S.B.; Philpott, K.L. Principles of early drug discovery. *British journal of pharmacology* **2011**, *162*, 1239-1249, <https://doi.org/10.1111/j.1476-5381.2010.01127.x>.
61. Sharma, A.; Datta, D.; Balasubramaniam, R. Molecular dynamics simulation to investigate the orientation effects on nanoscale cutting of single crystal copper. *Computational Materials Science* **2018**, *153*, 241-250, <https://doi.org/10.1016/j.commatsci.2018.07.002>.
62. Kunjiappan, S.; Pavadai, P.; Vellaichamy, S.; Ram Kumar Pandian, S.; Ravishankar, V.; Palanisamy, P.; Govindaraj, S.; Srinivasan, G.; Premanand, A.; Sankaranarayanan, M. Surface receptor-mediated targeted drug delivery systems for enhanced cancer treatment: A state-of-the-art review. *Drug Development Research* **2021**, *82*, 309-340, <https://doi.org/10.1002/ddr.21758>
63. Saravanan, K.S.; Arjunan, S.; Kunjiappan, S.; Pavadai, P.; Sundar, L.M. Phytoconstituents as Lead Compounds for Anti-Dengue Drug Discovery. In *Antiviral Drug Discovery and Development*; Springer: 2021; 159-193, https://doi.org/10.1007/978-981-16-0267-2_7.
64. Kumar, B.; Parasuraman, P.; Murthy, T.P.K.; Murahari, M.; Chandramohan, V. *In silico* screening of therapeutic potentials from *Strychnos nux-vomica* against the dimeric main protease (Mpro) structure of SARS-CoV-2. *Journal of Biomolecular Structure and Dynamics* **2021**, 1-19, <https://doi.org/10.1080/07391102.2021.1902394>.
65. Abdelrheem, D.A.; Ahmed, S.A.; Abd El-Mageed, H.; Mohamed, H.S.; Rahman, A.A.; Elsayed, K.N.; Ahmed, S.A. The inhibitory effect of some natural bioactive compounds against SARS-CoV-2 main protease: insights from molecular docking analysis and molecular dynamic simulation. *Journal of Environmental Science and Health, Part A* **2020**, *55*, 1373-1386, <https://doi.org/10.1080/10934529.2020.1826192>.
66. Rahman, A.; Anwar, K.N.; Fazal, F.; Malik, A.B. of July 3, 2020. RhoA/Rho-associated kinase pathway selectively regulates thrombin-induced intercellular adhesion molecule-1 expression in endothelial cells via activation of 1 B kinase and phosphorylation of RelA/p65. *J Immunol* **2004**, *173*, 6965-6972, <https://doi.org/10.4049/jimmunol.173.11.6965>.